Research Article

Enhanced magnetic properties of Fe-based nanocrystalline composites by addition of carbonyl iron powders

Liang Chang[1] · Yiqun Zhang[1,2] · Yaqiang Dong[1,2] · Qiang Li[3] · Aina He[1,2] · Chuntao Chang[4] · Xinmin Wang[1]

Abstract

Fe-based nanocrystalline/carbonyl iron hybrid soft magnetic composites (N/C HSMCs) with excellent comprehensive magnetic properties were fabricated by cold compaction of gas-atomized FeSiBPNbCu amorphous powder and carbonyl iron powder (CIP). Upon annealing at the optimum temperature, the N/C HSMCs demonstrated excellent magnetic properties including a high permeability range from 104 to 124, high-frequency stability up to 1 MHz, superior DC-bias permeability increase from 58 to 86% at a bias field of 50 Oe, and low core loss that regulated less than 1200 mW/cm^3 and reduced to as low as 732 mW/cm^3 at 100 kHz for $B_m = 0.1$ T. The ameliorative magnetic properties of the present N/C HSMCs can be attributed to the addition of CIP, which typically enhances the monolithic saturation magnetic flux density and rebuilds the chain structures in a more integrated formation. Further, the precipitation of an ultrafine α-Fe(Si) phase in the amorphous matrix and a uniform insulation layer covered with the powder were the foundation for numerous other superior performance results.

Keywords Nanocrystalline powder · Carbonyl iron powder · Hybrid soft magnetic composite · Excellent soft magnetic properties

1 Introduction

Soft magnetic composites (SMCs) have been widely used in noise suppressors, inductors, and other reactors in electromagnetic devices owing to their unique combination of properties, namely magnetic and thermal isotropy, high magnetic permeability, and extremely low power loss. The magnetic properties, characteristics, processing, and applications of SMCs aimed at achieving high frequency, miniaturization, and noise reduction have been widely studied in recent years [1, 2]. Hybrid SMCs (HSMCs), as they contain more than two constituent magnetic materials, have exhibited even greater performance and complex behavior than that of single SMCs. It can be designed flexibly by controlling the constituent magnetic materials; hence, the electrical and magnetic properties of HSMCs can be tailored, within their physical limits, to the specific requirements of the application, i.e., allowing the alteration of the permeability or DC-bias property of the composite over a wide range and leading to an increase in magnetic stability [3].

Fe-based nanocrystalline alloys with excellent soft magnetic properties were widely studied [4, 5]; these can serve as a matrix or filler for the production of high-performance HSMCs, and numerous studies have reported using Fe-based nanocrystalline alloy powders [6, 7]. In our previous work, the FeSiBPNbCu nanocrystalline SMCs using gas-atomized powder were prepared and the characteristics

SN Applied Sciences
A SPRINGER NATURE journal

of the corresponding properties at high frequency were studied [8]. However, it is more difficult to achieve high density in Fe-based alloys owing to the high hardness; even the gas-atomized FeSiBPNbCu powders are spherical in shape. Further, to reduce the eddy current loss, gas-atomized powders are separated by an electric insulation layer. This typically results in low saturation magnetization (B_s) for the SMCs. Considering these issues, the soft magnetic properties of FeSiBPNbCu nanocrystalline SMCs could be optimized by doping with another soft magnetic material [9–11].

Carbonyl iron powder (CIP) is considered as a candidate constituent material because of its low cost, high B_s, and high complex permeability [12–14]. It is useful for increasing the density owing to its large plastic deformation under pressure during compaction and consequently improves the permeability of HSMCs. Furthermore, as a microwave absorption material, the high resonance frequency of CIP, which can range up to the G-hertz level, can enhance the high-frequency stability of the permeability. Finally, the high B_s achieved with compositing with CIP is conducive to miniaturization, resulting in a superior DC-bias property for HSMCs, which is a benefit for their application in large direct current fields. Thus, in the present work, Fe-based nanocrystalline/carbonyl iron hybrid soft magnetic composites (N/C HSMCs) are fabricated by FeSiBPNbCu gas-atomized spherical powder with a fully amorphous phase and CIP with high B_s. The N/C HSMCs are fabricated by cold compaction and then annealed under the appropriate conditions. The magnetic properties of the resulting N/C HSMCs are investigated systematically.

2 Materials and methods

Multicomponent FeSiBPNbCu ingot was prepared by induction melting of a mixture of high-purity metals in a high-purity argon atmosphere. The FeSiBPNbCu ingots were remelted under vacuum in a quartz tube using an induction-heating coil, injected through a nozzle with a diameter of 0.8 mm and atomized by high-pressure argon gas with a dynamic pressure of 7 MPa. Metallic powder, sieving out the particle size below 75 μm, with a fully amorphous phase prepared by gas atomization method. The corresponding FeSiBPNbCu gas-atomized amorphous powder, with a mass fraction of the HSMCs that regulated within a certain range of 0–50 wt%, was substituted by CIP with an average particle size of 5 μm. The characteristics of CIP were examined by X-ray diffraction (XRD) with CuKα radiation and scanning election microscopy (SEM). The two powders were uniformly mixed with 2 wt% epoxy resin as an organic binder and then dried for 30 min in an electric thermostatic drying oven. Toroid-shaped

FeSiBPNbCu amorphous/CIP HSMCs with an outer diameter of 20.3 mm, an inner diameter of 12.7 mm and a height of 5 mm were fabricated by cold pressing under a pressure of 1800 MPa at room temperature. Then, the compacted cores were annealed at 480 °C for 0.5 h in vacuum atmosphere to nanocrystallization and reduce the internal stress caused by pressing. The specimens were marked as S_x ($x = 0$, 10, 20, 30, 40, 50, representing the mass fraction of CIP). The density of the samples was determined by the Archimedes immersion method using distilled water as the working liquid. The morphology of the N/C HSMCs was analyzed by SEM. The M–H loops of the N/C HSMCs were measured using a vibrating sample magnetometer (VSM). The permeability was calculated from the core inductance, which was measured by an Agilent 4294A impedance analyzer from 1 kHz to 110 MHz. The DC-bias field performance was measured by an Agilent 4284A LCR meter. The total core loss was measured by an alternating current (AC) B–H loop analyzer.

3 Results and discussion

Figure 1 displays the XRD pattern of the CIP. Three diffraction peaks attributed to the (110), (200), and (211) lattice planes of the α-Fe phase appear in the XRD patterns of the CIP within the sensitivity of XRD measurement. The inset of Fig. 1 displays the morphology of the CIP with the particle size ranging up to 5 μm. The powder is spherical in shape, which is more favorable for the separation and a uniform insulation coating, thereby reducing the eddy current loss between the powders.

The morphology of the cross section of the N/C HSMCs is displayed in Fig. 2. It can be observed that the cross section of the N/C HSMCs indicates a clear difference for the
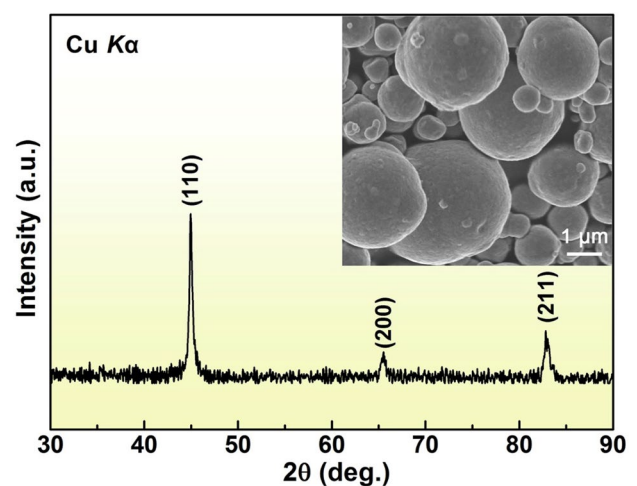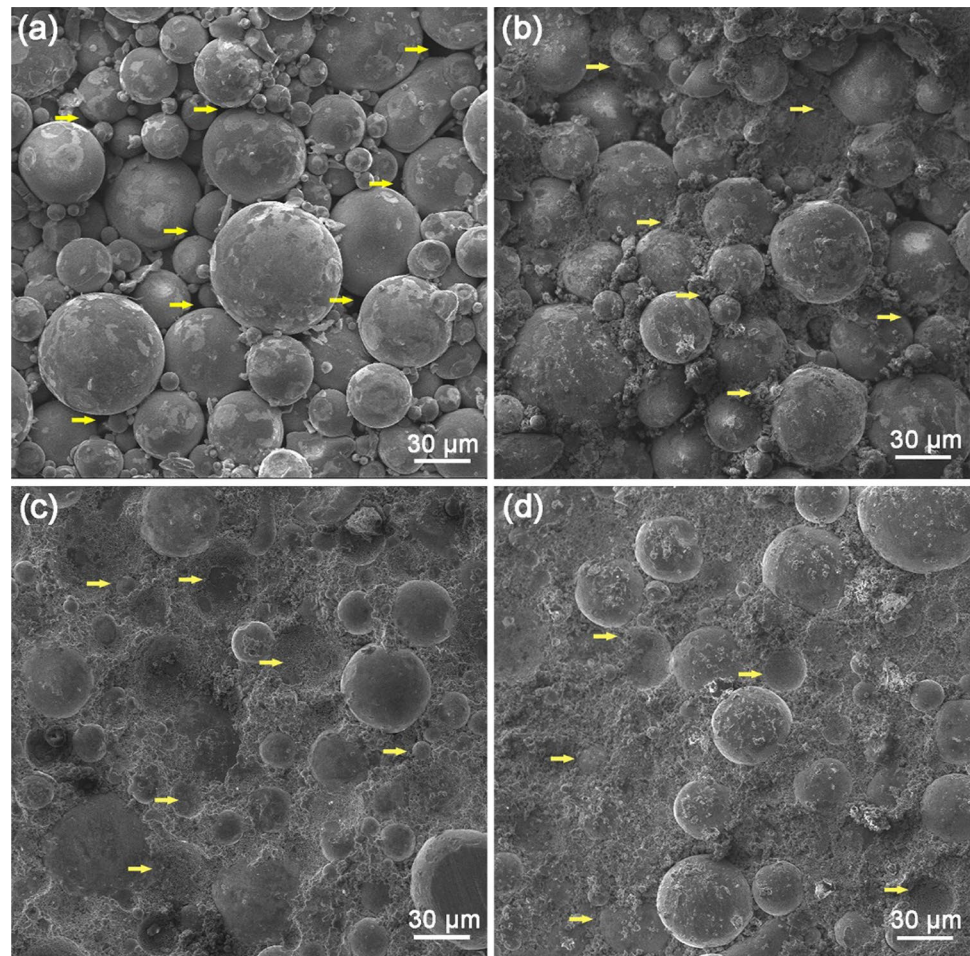

Fig. 1 XRD patterns of CIP; inset displays morphology of CIP

Fig. 2 Section morphology of N/C HSMCs: **a** S_0, **b** S_{10}, **c** S_{30}, and **d** S_{50}

composites with a different mass fraction of CIP. Figure 2a displays the morphology of N/C HSMCs, S_0. Although the FeSiBPNbCu gas-atomized powder exhibits a wide particle size distribution, it can be observed from the labeled area that a gap remains between the particles, which can reduce the density of the SMCs. When the composite mass fraction is 10 wt%, as displayed in Fig. 2b, a CIP with a small particle size filled in the gaps commendably, resulting in an increase in the density, thus typically improving the performance of the N/C HSMC. Figure 2c and d indicates that the FeSiBPNbCu gas-atomized powders are separated and can even be regarded as embedded in the massive CIP when the mass fraction increases to 30 and 50 wt%. In conclusion, the density of N/C HSMCs is increased, to the range 5.38–6.49 g/cm³, as the mass fraction of the CIP increases from 0 to 50 wt%, which has a gradual influence on the magnetic properties of the N/C HSMCs.

Figure 3 displays the frequency dependence of the permeability for the N/C HSMCs. The permeability is clearly improved as the mass fraction of the composited CIP is 10–50 wt%. In particular, the S_{10} exhibits the highest initial permeability of 124 and retains a stable permeability of
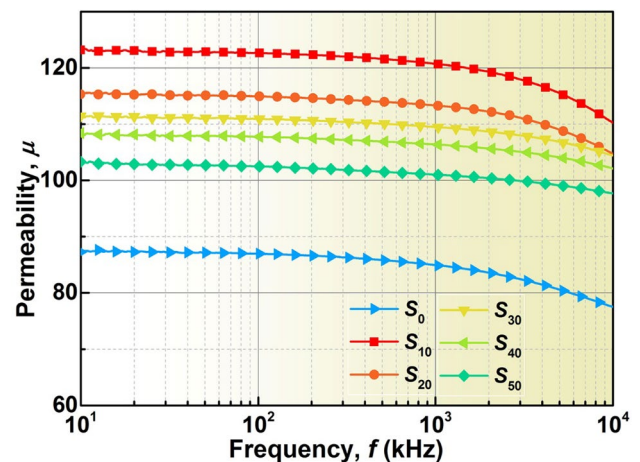

Fig. 3 Frequency dependence of permeability for N/C HSMCs

120 up to 1 MHz. Then, the permeability decreases gradually as the mass fraction of the CIP increases to 50 wt%; however, it continues to indicate a significant increase compared with that of 0 wt%. In the previous research,

it was concluded that the static magnetic interactions among the inclusion particles embedded in the matrix have critical roles in determining the composite properties, where the sensitively depends on the inclusion particle arrangement and, especially, chain structure. The chain structures exhibit strong effective susceptibility anisotropy despite the fact that all the constituent components are isotropic [15]. Thus, the enhancement of the magnetic permeability mainly owning to the improvement of the internal chain structure in SMCs. Meanwhile, it can be observed from Fig. 2 that the CIP with a smaller particle size filled in the original gap position, which amounted to a reduction in the mass fraction of the non-magnetic material. This supplemented the density of the N/C HSMCs, and consequently, the internal chain structure could be rebuilt in a more integrated fashion, as well as significantly increasing the magnetic permeability. Subsequently, a new type of air gap with smaller volume produced by the increasing mass fraction of the CIP, resulting in large porosity, which could prevent the propagation of domain movement among the particles in the magnetizing process and reducing the permeability [16]. Moreover, the relaxation frequency continued to move to high frequency with the increased mass fraction of the CIP; all specimens exhibited excellent high-frequency stability up to approximately 1 MHz, or more.

Figure 4 presents the frequency dependence of the core loss for the N/C HSMCs at the introduction level of 0.1 T. In general, the total core loss (P_{cv}) includes hysteresis loss (P_h), eddy current loss (P_e), and residual loss (P_r). The P_r is a combination of relaxation and resonant losses of the system, which is important only at extremely low induction levels and high frequencies and can be ignored in power applications. Then, the core loss of the MPCs is expressed as the sum of P_h and P_e provided changes in the magnetic field inside the material are not accompanied by relaxation phenomena (e.g., magnetic

resonance) [17]. P_e is dominant in the high-frequency range and can be described as follows [18, 19]:

$$P_e = \frac{CB^2 f^2 d^2}{\rho} \tag{1}$$

where C is the proportionality constant, B is the magnetic flux density, f is the frequency, ρ is the resistivity, and d is the thickness of the material. Thus, the P_e of N/C HSMCs could increase with the addition of CIP with low resistivity; however, this is not the case in practice. As indicated in Fig. 4, the P_{cv} of the specimens was less than that of 0 wt%, even with the increasing in the mass fraction of the CIP from 10 to 40 wt%. In particular, S_{10} exhibited the least core loss of 732 mW/cm^3 at 100 kHz. It can be concluded that CIP contains a smaller particle size, resulting in less P_{cv} compared with the corresponding substituted FeSiBPN-bCu powder and the influence of particle size on P_{cv} is considerably greater than that of low resistivity. The effect of resistivity grows gradually as the increased mass fraction of CIP increases to 50 wt%; the overall loss of 1160 mW/cm^3 is marginally greater than that of 0 wt% (1025 mW/cm^3), which indicates that the effect of resistivity is more prominent, although the particle size is small and the unit volume loss is low. Further, all specimens exhibited low overall loss owing to the uniform insulation layers coated on the powder surface, which provides a relatively high resistivity and can effectively reduce the P_e.

The DC level must be tolerated for SMCs in many applications; hence, the SMCs must exhibit a high incremental permeability (μ_Δ) (also known as reversible permeability μ_{rev} when the AC magnetic field is small) in a higher DC-bias magnetic field H_{DC} (the so-called DC-bias property) [20, 21]. When DC flows through the winding of a ferromagnetic device, it tends to pre-magnetize the
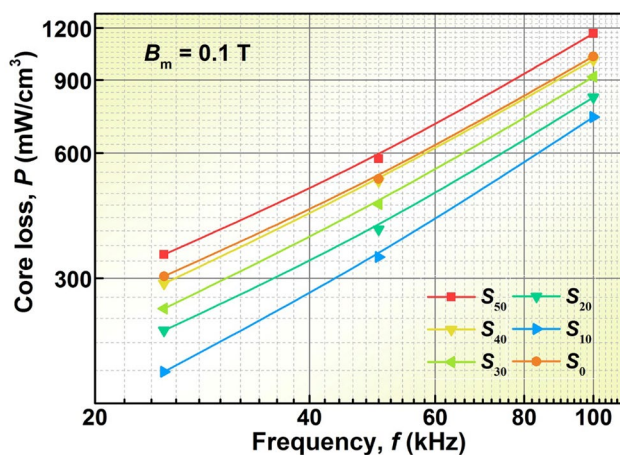

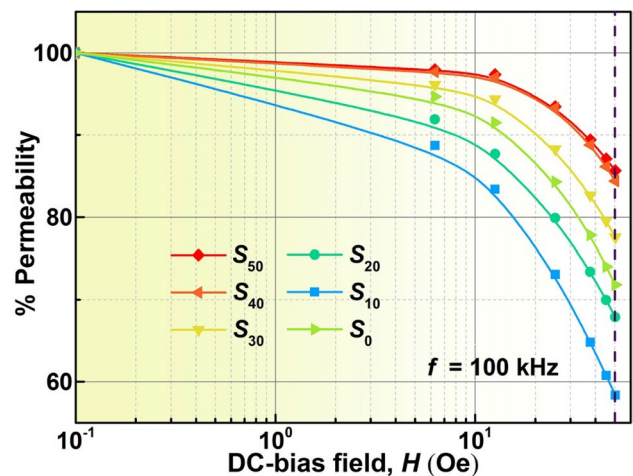**Fig. 4** Frequency dependence of core loss for N/C HSMCs

Fig. 5 Percentage of permeability with DC-bias field at 100 kHz for N/C HSMCs

Fig. 6 *M–H* loop of the N/C HSMCs S_0, S_{10}, S_{30}, and S_{50}
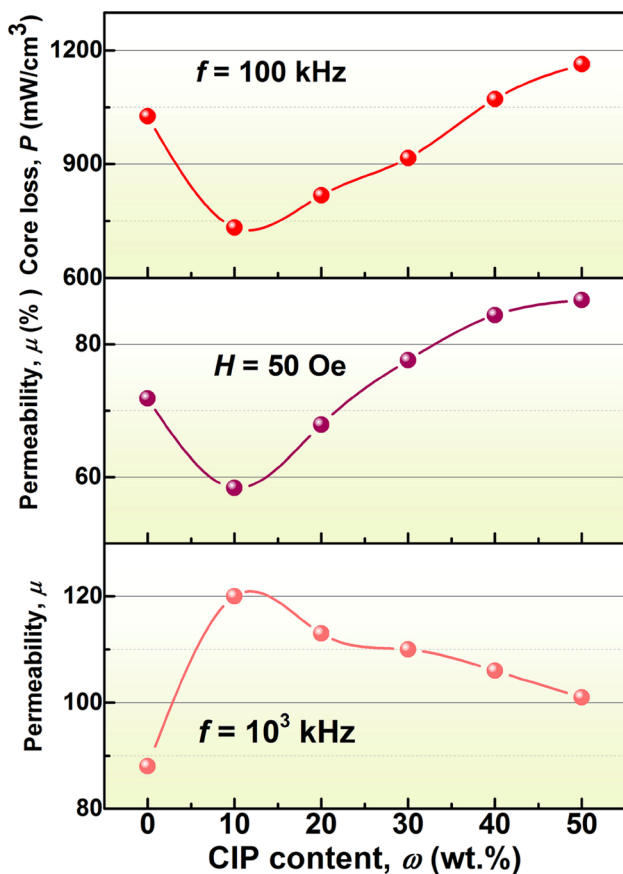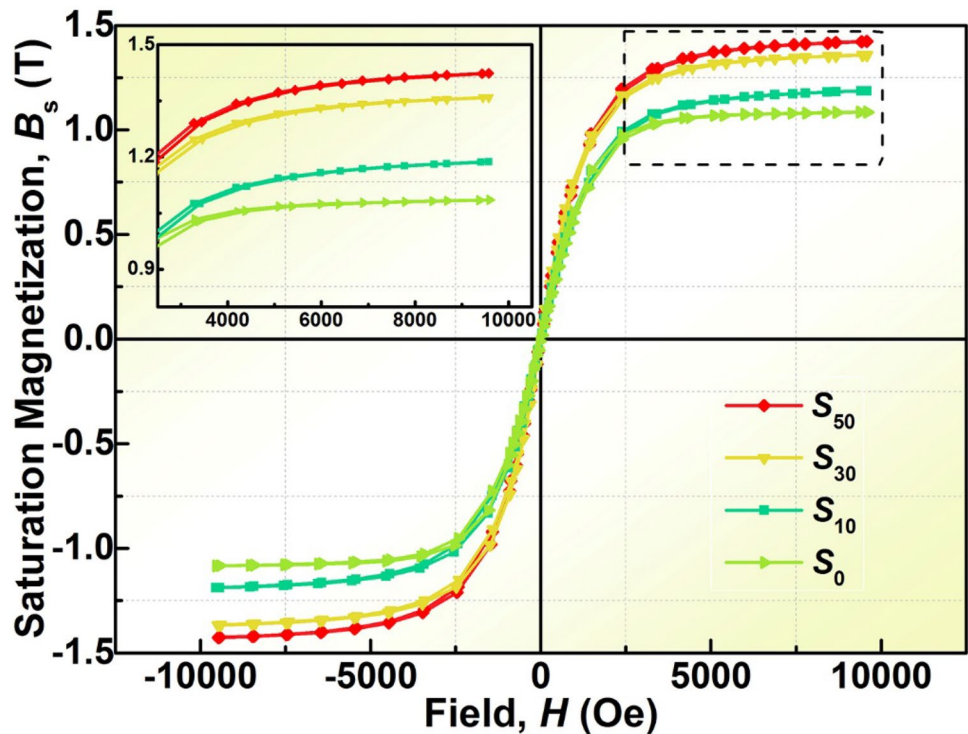

Fig. 7 Effect of CIP with different mass fractions on various performances of N/C HSMC

SMCs and reduce their inductance. This permeability is referred to as the incremental permeability μ_Δ and defined as [17]:

$$\mu_\Delta = \frac{1}{\mu_0}\left[\frac{\Delta B}{\Delta H}\right]H_{DC} \tag{2}$$

where μ_0 is the vacuum permeability, ΔB is the incremental flux density, and ΔH is the incremental field intensity. The inductance progressively decreases as the DC-bias field increases and the SMCs approach saturation.

The DC-bias field dependence of the percent permeability for the N/C HSMCs at 100 kHz is displayed in Fig. 5. As can be observed, the percent of permeability of S_0 remains at 72% at $H = 50$ Oe, and the characteristic of S_{10}–S_{50} increases gradually. In particular, S_{50} exhibits the highest μ_Δ of 86%. Hence, it is possible to improve the DC-bias performance by compositing with an appropriate mass fraction of CIP, which, due mainly to the improved B_s of the specimens, makes it considerably more difficult to approach saturation.

As can be observed from Fig. 6, the characteristic of B_s drifts in an approximately similar fashion as the μ_Δ, and the B_s of S_{30} and S_{50} increases to 1.35 and 1.42 T compared with S_0 (1.1 T), respectively, which means that it should require a greater H_{DC} to approach saturation compared with S_0; of course, the premise is that they have a similar ΔB. Moreover, the additional air gaps in the N/C HSMCs can pin the domain wall in the magnetizing process and prevent the propagation of domain movement among the

Table 1 Comparison of permeability, core loss, and DC-bias between our newly developed N/C HSMCs and the typical SMCs reported previously

Specimens	Permeability	Core loss (mW/cm^3)		DC-bias (%)
	$f = 1$ MHz	0.05 T/100 kHz	0.1 T/100 kHz	50 Oe
S_{10}	120	201	732	58
S_{30}	110	224	916	77
S_{50}	102	280	1160	86
FeSiBNbCu [7]	40	–	1050	67
FeSiBNbCu [22]	93	–	1030	43
FeSiAl [23]	55	–	600	76
FeSiBPNb [24]	45	–	1770	95
FeSiBP@(NiZn)Fe$_2$O$_4$ [25]	70	–	1100	–
Fe@Fe$_3$O$_4$@ESR [26]	85	651	–	–
Fe@Fe$_3$O$_4$ [27]	88	688	–	–

particles and consequently suppress the decrease in the permeability, achieving a high percent permeability.

Figure 7 presents the effect of the CIP with different mass fractions on different performances of the N/C HSMCs. Certainly, the addition of CIP would appear to be beneficial to the optimization of the soft magnetic performances for N/C HSMCs. The permeability of the overall specimen is significantly improved; in particular, S_{10} exhibits the highest effective permeability of 120 at $f = 1$ MHz. This is mainly due to the consummation of the magnetic circuit as the CIP is added. The P_{cv} of the overall specimen does not increase significantly; conversely, it decreases when the mass fraction of CIP ranges from 10 to 30 wt%, which indicates that the reduction in particle size is beneficial to decrease the P_{cv} under an excellent insulation precondition. A certain amount of CIP (30–50 wt%) increases the B_s and consequently improves the DC-bias performance, which indicates that the specimens, within a high flux increment under the applied magnetic field, do not easily approach saturation. That is, high permeability and excellent DC-bias performance can be achieved simultaneously.

Table 1 summarizes the soft magnetic properties of the present S_{10}, S_{30}, S_{50} and the typical SMCs reported previously. It can be seen that the N/C HSMCs fabricated in this work exhibit rather better comprehensive properties than those of the previously reported SMCs, which can better meet the development direction of miniaturization and high frequency of electronic components in the near future.

4 Conclusions

The magnetic properties of N/C HSMCs fabricated using FeSiBPNbCu gas-atomized powder and CIP were investigated. Consequently, we provided a novel type of SMC that contained a large selection interval for the comprehensive performance including high initial permeability, superior DC-bias, and low core loss, which means that additional options are provided for future practical applications. Based on the results in this study, it can be concluded that adding the proper content of CIP with small average particle diameter can enhance the B_s and facilitate the rebuilding of the chain structures in a more integrated fashion. This is an effective approach to improve the comprehensive soft magnetic properties of SMCs.

Compliance with ethical standards

Conflicts of interest The authors declare that they have no conflict of interest.

References

1. Oh KK, Lee H, Lee WS, Yoo MJ, Kim WN, Yoon HG (2009) Effect of viscosity on the magnetic permeability of Sendust-filled polymer composites. J Magn Magn Mater 321:1295–1299
2. Fan XA, Wu ZY, Li GQ, Wang J, Xiang ZD, Gan ZH (2016) High resistivity and low core loss of intergranular insulated Fe–6.5wt.%Si/SiO$_2$ composite compacts. Mater Des 89:1251–1258
3. Pittini-Yamada Y, Périgo EA, De Hazan Y, Nakahara S (2011) Permeability of hybrid soft magnetic composites. Acta Mater 59:4291–4302
4. Inoue A, Shen BL (2003) Soft magnetic properties of nanocrystalline Fe–Co–B–Si–Nb–Cu alloys in ribbon and bulk forms. J Mater Res 18:2799–2806
5. Ohta M, Yoshizawa Y (2007) Magnetic properties of nanocrystalline Fe$_{82.65}$Cu$_{1.35}$Si$_x$B$_{16-x}$ alloys ($x = 0–7$). Appl Phys Lett 91:062513–062517
6. Kim GH, Noh TH, Choi GB, Kim KY (2003) Magnetic properties of FeCuNbSiB nanocrystalline alloy powder cores using ball-milled powder. J Appl Phys 93:7211–7213

7. Kim TH, Jee KK, Kim YB, Byun DJ, Han JH (2010) High-frequency magnetic properties of soft magnetic cores based on nanocrystalline alloy powder prepared by thermal oxidation. J Magn Magn Mater 322:2423–2427

8. Chang L, Xie L, Liu M, Li Q, Dong YQ, Chang CT, Wang XM, Inoue A (2018) Novel Fe-based nanocrystalline powder cores with excellent magnetic properties produced using gas-atomized powder. J Magn Magn Mater 452:442–446

9. Périgo EA, Nakahara S, Pittini-Yamada Y, De Hazan Y, Graule T (2011) Magnetic properties of soft magnetic composites prepared with crystalline and amorphous powders. J Magn Magn Mater 323:1938–1944

10. Kim HJ, Nam SK, Kim KS, Yoon SC, Sohn KY, Kim MR, Song YS, Park WW (2012) Magnetic properties of amorphous Fe–Si–B powder cores mixed with pure iron powder. J Appl Phys 51:103001

11. Füzerová J, Füzer J, Kollár P, Hegedüs L, Bureš R, Fáberová M (2012) Analysis of the complex permeability versus frequency of soft magnetic composites consisting of iron and $Fe_{73}Cu_1Nb_3Si_{16}B_7$. IEEE Trans Magn 48:1545–1548

12. Xu Y, Luo J, Yao W, Xu J, Li T (2015) Preparation of reduced graphene oxide/flake carbonyl iron powders/polyaniline composites and their enhanced microwave absorption properties. J Alloys Compd 636:310–316

13. Liu QC, Zi ZF, Zhang M, Pang AB, Dai JM, Sun YP (2013) Enhanced microwave absorption properties of carbonyl iron/Fe_3O_4 composites synthesized by a simple hydrothermal method. J Alloys Compd 561:65–70

14. Yang RB, Tsay CY, Hung DS, Liang WF, Yao YD, Lin CK (2009) Complex permittivity and permeability of iron-based composite absorbers measured by cavity perturbation method in X-band frequency range. J Appl Phys 105:07A528

15. Wang JJ, Song Y, Ma XQ, Chen LQ, Nan CW (2015) Static magnetic solution in magnetic composites with arbitrary susceptibility inhomogeneity and anisotropy. J Appl Phys 117:043907

16. Dong YQ, Li ZC, Liu M, Chang CT, Li FS, Wang XM (2017) The effects of field annealing on the magnetic properties of FeSiB amorphous powder cores. Mater Res Bull 96:160–163

17. Liu YP, Yi YD, Shao W, Shao YF (2013) Microstructure and magnetic properties of soft magnetic powder cores of amorphous and nanocrystalline alloys. J Magn Magn Mater 330:119–133

18. Serpico C, Visone C, Mayergoyz ID, Basso V, Miano G (2000) Eddy current losses in ferromagnetic laminations. J Appl Phys 87:6923–6925

19. Shokrollahi H, Janghorban K (2007) Soft magnetic composite materials (SMCs). J Mater Process Technol 189:1–12

20. Ott G, Wrba J, Lucke R (2003) Recent developments of Mn–Zn ferrites for high permeability applications. J Magn Magn Mater 254:535–537

21. Zaspalis VT, Tsakaloudi V, Kolenbrander M (2007) The effect of dopants on the incremental permeability of MnZn-ferrites. J Magn Magn Mater 313:29–36

22. Choi HY, Ahn SJ, Noh TH (2004) Magnetic properties of nanocrystalline $Fe_{73.5}Cu_1Nb_3Si_{15.5}B_7$ alloy powder cores with different particle size prepared by rotor mill. Phys Stat Sol A 201:1879–1882

23. Liu HJ, Su HL, Geng WB, Sun ZG, Song TT, Tong XC, Zou ZQ, Wu YC, Du YW (2016) Effect of particle size distribution on the magnetic properties of Fe–Si–Al powder core. J Supercond Nov Magn 29:463–468

24. Guo JJ, Dong YQ, Man QK, Li Q, Chang CT, Wang XM, Li RW (2016) Fabrication of FeSiBPNb amorphous powder cores with high DC-bias and excellent soft magnetic properties. J Magn Magn Mater 401:432–435

25. Li XL, Dong YQ, Liu M, Chang CT, Wang XM (2017) New Fe-based amorphous soft magnetic composites with significant enhancement of magnetic properties by compositing with nano-(NiZn) Fe_2O_4. J Alloys Compd 696:1323–1328

26. Zhao GL, Wu C, Yan M (2017) Evolution of the insulation matrix and influences on the magnetic performance of Fe soft magnetic composites during annealing. J Alloys Compd 685:231–236

27. Zhao GL, Wu C, Yan M (2016) Enhanced magnetic properties of Fe soft magnetic composites by surface oxidation. J Magn Magn Mater 399:51–57